Equilibrium Distribution of Permeants in Polyelectrolyte Microcapsules Filled with Negatively Charged Polyelectrolyte: The Influence of Ionic Strength and Solvent Polarity

Weijun Tong,[†,‡] Haiqing Song,[§] Changyou Gao,*[,†] and Helmuth Möhwald[‡]

Department of Polymer Science and Engineering, and Key Laboratory of Macromolecule Synthesis and Functionalization, Ministry of Education, and The College of Management, Zhejiang University, Hangzhou 310027, China, and Max-Planck-Institute of Colloids and Interfaces, 14424 Potsdam, Germany

Received: September 16, 2005; In Final Form: April 13, 2006

The effects of ionic strength and solvent polarity on the equilibrium distribution of fluorescein (FL) and FITC−dextran between the interior of polyelectrolyte multilayer microcapsules filled with negatively charged strong polyelectrolyte and the bulk solution were systematically investigated. A negatively charged strong polyelectrolyte, poly(styrene sulfonate) (PSS), used for $CaCO_3$ core fabrication, was entrapped inside the capsules. Due to the semipermeability of the capsule wall, a Donnan equilibrium between the inner solution within the capsules and the bulk solution was created. The equilibrium distribution of the negatively charged permeants was investigated by means of confocal laser scanning microscopy as a function of ionic strength and solvent polarity. The equilibrium distribution of the negatively charged permeants could be tuned by increasing the bulk ionic strength to decrease the Donnan potential. Decreasing the solvent polarity also could enhance the permeation of FL, which induces a sudden increase of permeation when the ethanol volume fraction was higher than 0.7. This is mainly attributed to the precipitation of PSS. A theoretical model combining the Donnan equilibrium and Manning counterion condensation was employed to discuss the results.

Introduction

In recent years, polyelectrolyte multilayer microcapsules prepared by layer-by-layer (LbL) assembly of oppositely charged polyelectrolytes onto removable colloidal particles have received much attention because of scientific interest and their technological importance.[1] These novel hollow capsules have shown potential applications as drug delivery vehicle, biosensors, and microreactors as well as microcarriers.[2] For various applications a critical question is how to control the loading and subsequent release of diverse substances into/from the microcapsules in a desired manner. Therefore, many efforts have been devoted to controlling the permeability of the capsules. The permeability of the polyelectrolyte microcapsules can be controlled by layer number,[3] wall cross-linking,[4] pH value,[5] ionic strength,[6] and polarity of the solution,[7] as well as annealing[8] and resealing[9] after core removal. Moreover, electrostatic interaction between the capsules and the substances in bulk solution has also been found to exhibit a pronounced influence on the loading capability of the polyelectrolyte microcapsules.[10]

We reported previously that multilayer microcapsules containing free poly(styrene sulfonate) (PSS) showed very sensitive selectivity to the charge sign of the permeants.[11] These capsules are templated on PSS-doped $CaCO_3$ microparticles and contain simultaneously the negatively charged PSS upon core removal. (Scheme 1) They repel completely fluorescent probes with negative charges but attract positively charged species. This selectivity is even sensitive to dextran ($M_w \sim 70$ kDa) labeled with only few charged dyes. In principle, the semipermeability of the capsule wall and the encapsulated polyelectrolytes could be used to create a difference in the chemical composition between the bulk solution and the capsule interior, which is the well-known Donnan equilibrium.[12] As a result, the equilibrium distribution of small charged permeants will also be determined. Although our preliminary results have demonstrated the unique properties, detailed studies are still required to explore the equilibrium distribution of small charged permeants in response to environmental stimuli such as ionic strength and polarity of solvent, because this is an intriguing issue concerning possible applications of the microcapsules as microreactors or microcarriers.

SCHEME 1: Schematic Illustration To Show the Topology of the as-Prepared Microcapsules

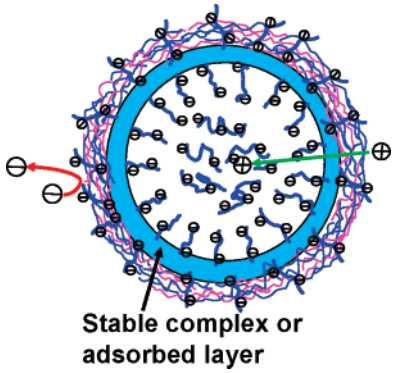

Therefore, these factors will be elucidated in this paper to precisely identify their influence, taking both small dye molecules and macromolecular permeants. In this paper, we encapsulate a negatively charged polyelectrolyte into the capsules and measure the inner concentration change of a dye permeant depending on the ionic strength and solvent polarity of the solution. Confocal laser scanning microscopy (CLSM)

* Corresponding author. Tel: +86-571-87951108. Fax: +86-571-87951948. E-mail: cygao@mail.hz.zj.cn.
[†] Department of Polymer Science and Engineering, Zhejiang University.
[‡] Max-Planck-Institute of Colloids and Interfaces.
[§] The College of Management, Zhejiang University.

10.1021/jp055258w CCC: $33.50
Published on Web 06/09/2006

is used to measure the permeant concentration by using the average ratio of the fluorescence intensity emitted from interior and exterior of the capsules. Thus we show that the concentration mainly depends on the Donnan equilibrium and less on the wall permeability. The specific interactions (e.g., hydrophobic) between the permeants and the encapsulated polyelectrolytes may also play an important role in the permeant distribution.

Experimental Section

Materials. Sodium poly(styrene sulfonate) (PSS, $M_w \sim 70$ kDa), poly(allylamine hydrochloride) (PAH, $M_w \sim 65$ kDa), calcium nitrate tetrahydrate ($Ca(NO_3)_2 \cdot 4H_2O$), sodium carbonate (Na_2CO_3), disodium ethylenediaminetetraacetate dihydrate (EDTA), rhodamine 6G (Rd6G), fluorescein sodium (FL), FITC−dextran ($M_w \sim 4$ kDa), and tetramethylrhodamine isothiocyanate-labeled dextran (TRITC−dextran, $M_w \sim 4.4$ kDa) were all obtained from Sigma-Aldrich. All compounds were used as received. The water used in all experiments was prepared in a three-stage Millipore Milli-Q Plus 185 purification system and had a resistivity higher than 18.2 MΩ.

Methods. Fabrication of $CaCO_3$ Particles. To prepare the $CaCO_3$ particles, PSS was completely dissolved in 200 mL of 0.025 M calcium nitrate solution in a beaker under magnetic agitation (~600 rpm), into which an equal volume of 0.025 M sodium carbonate solution in another beaker was rapidly poured at room temperature. The final PSS concentration was 2 mg/mL. At the end of the reaction, the precipitated $CaCO_3$ particles were collected and washed using a membrane filtration apparatus equipped with a cellulose filter having pore size of 0.45μm. The average size of the obtained particles is 8.2 ± 0.8 μm, which is measured and averaged from more than 100 particles by CLSM.

Layer-by-Layer Coating and Capsule Fabrication. Alternating adsorption of polyelectrolytes (2 mg/mL) onto the $CaCO_3$ microparticles (~1% w/w in suspension) was conducted in 0.5 M NaCl solution for 10 min followed by three washings in water. After assembly of five polyelectrolyte bilayers, the coated particles were incubated in 0.02 M EDTA (pH 7) solution for 30 min under shaking. The resultant capsules were centrifuged at 1500*g* for 5 min with three washings in fresh EDTA solution. Finally, the capsules were washed three times with water. As the PSS-doped $CaCO_3$ particles possess negatively charged surfaces, the first layer was PAH, while the outermost layer in this study was always PSS.

Confocal Laser Scanning Microscopy (CLSM). Confocal images were taken with a Leica confocal scanning system mounted to a Leica Aristoplan and equipped with a 100× oil immersion objective with a numerical aperture (NA) of 1.4.

The capsules were incubated overnight in a solution with a given ionic strength or solvent polarity. Equal amounts of capsule suspension and probe solution with the same solution conditions were mixed. Pictures were taken after 10 min. The concentrations of FL and dextran were fixed at 0.2 and 2 mg/mL in all measurements, respectively.

For quantitative analysis, the fluorescence intensity from the capsule interior (I_{int}) and the bulk solution (I_0) was measured by the CLSM software. The ratio of I_{int}/I_0 was calculated and averaged from more than 30 capsules of a same sample. During the measurement, the settings of the CLSM were constant.

Statistical Analysis. Statistical analysis of the data was performed using the two-population Student's *t*-test. The significant level was set as $P < 0.05$.

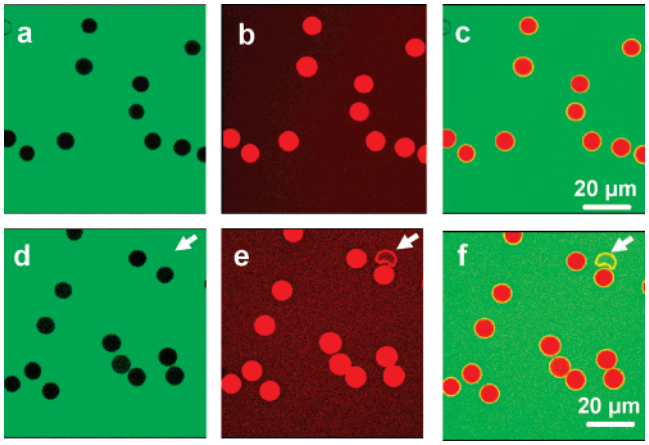

Figure 1. CLSM images of the capsules incubated in a Rd6G and FL mixed solution (a−c) and in a TRITC−dextran and FITC−dextran mixed solution (d−f). Samples for a and d were excited at 488 nm (for FITC and FL), while those for b and e were excited at 543 nm (for Rd6G and TRITC). The overlapped images of a/b and d/e are shown in c and f, respectively.

Results and Discussion

Permeation Selectivity with Respect to the Charge Sign of the Permeants. The $CaCO_3$ particles used as templates were prepared in the presence of PSS, a negatively charged polyelectrolyte. As reported previously,[11] the PSS molecules are incorporated into the particles and part of them are entrapped in the hollow capsules after core removal. The capsules show very strong and sensitive selectivity to the permeation of permeants with different charge sign, as demonstrated in Figure 1. In a mixed solution of fluorescein (FL, negatively charged) and rhodamine 6G (Rd6G, positively charged), only Rd6G could permeate into the interiors of the hollow capsules (Figure 1b,c), while FL could not (Figure 1a,c). This behavior is even sensitive to the few charged chromophores in a labeled macromolecule such as dextran. Labeled dextran has a corresponding weak charge brought by the chromophores such as FITC (negatively charged) or TRITC (positively charged). Consequently, substantially different permeation was observed dependent on the charge sign of the very few chromophores per polymer. FITC−dextran was completely excluded (Figure 1d,f), while TRITC−dextran accumulated inside (Figure 1e,f). It is worth mention that the capsules having the same fluorescence intensity for the interior and exterior (Figure 1d,e,f, indicated by the arrows) are broken and no PSS is entrapped inside. Undoubtedly, this phenomenon should be attributed to the negatively charged PSS inside the capsules, which creates a Donnan equilibrium between the bulk solution and the interiors of the capsules, effecting a passive distribution of charged permeants. The equilibrium processes for low molecular weight permeants and dextran with a molecular weight of 4 kDa are so fast that 10 min is enough to reach the equilibrium state, and this state remains almost unchanged after 1 month.

Ionic Strength Dependence. Since increasing the ionic strength will decrease the Donnan potential, and hence decrease the concentration gradients of the permeants, addition of salt to the capsule suspension was first considered to tune the equilibrium distribution of the permeants. It is worth mentioning that for such a strong polyelectrolyte like PSS (Manning parameter $q_0 = l_B/l = 2.7$. Here l is the average distance of neighboring charges along the polyelectrolyte backbone before condensation and l_B is the Bjerrum length), the counterion condensation should be considered,[13] which will lower the

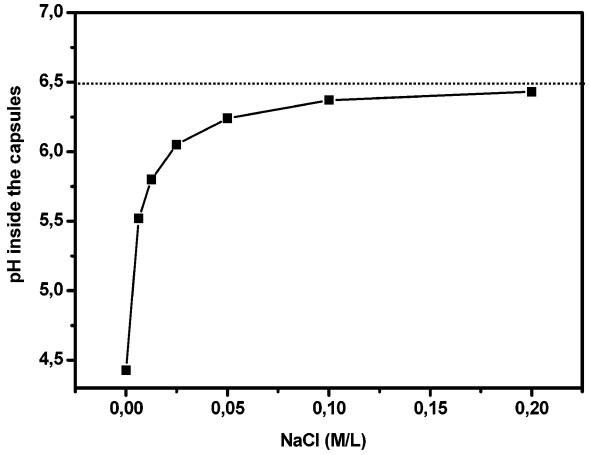

Figure 2. The calculated pH value inside the capsules as a function of bulk NaCl concentration according to a simple Donnan equilibrium model described in ref 12b with the realistic parameters: $c_{PSS} = 0.165$ M;[11] net charge fraction due to counterion condensation, $\theta = 0.38$; $pH_{bulk} = 6.5$. The dashed line represents the pH of the bulk solution.

charge density of PSS and thus decrease the Donnan potential. According to Hackl and Blagoi,[14] the fraction of net charge on the polyelectrolyte after the counterion condensation is given as

$$\theta = \frac{1}{Zq_0} = \frac{4\pi\epsilon_0\epsilon k_B T l}{Ze^2} \quad (1)$$

ϵ_0 and ϵ are the permittivity of a vacuum and the dielectric constant of the solvent, respectively. k_B is the Boltzman constant, T is the Kelvin temperature, Z is the valence of the counterion, and e is the elementary charge. At room temperature, for PSS ($l = 0.27$ nm) in the current case

$$\theta \approx 4.8 \times 10^{-3}\epsilon \quad (2)$$

Here, if we assume that the $\epsilon = 78.5$ is constant, the fraction of charged groups along PSS backbone should be 0.38. In the following calculations, the fraction of the PSS net charge at different dielectric constants is used according to eq 2.

One should also notice that FL as well as FITC is pH sensitive. In the current case, the Donnan equilibrium may cause a lower pH inside the capsules compared with that of the bulk solution. Here we can estimate the inner pH as a function of salt concentration from a simple model of the Donnan equilibrium of the small ions across the semipermeable capsule walls described in the literature[12b] using realistic parameters and taking the counterion condensation into account. The pH inside the capsules as a function of bulk NaCl concentration is shown in Figure 2. Basically, the salt concentration used in our experiments is in the range of 6.25−200 mM, which induces the inner pH to change from 5.5 to 6.4. Within this pH range, most FL molecules are in anion form[15] and the pH influence on the fluorescence intensity is negligible. So the ratio of I_{int}/I_0 (fluorescence from interior to bulk) can be used to estimate the equilibrium distribution of the permeants.

The ratio of I_{int}/I_0 as a function of NaCl concentration is illustrated in Figure 3. (All the data have significant differences with $P < 0.05$.) Fluorescence images, as depicted in the insets of Figure 3, were recorded at each NaCl concentration after mixing the capsule suspension and FL solution for 10 min and were used to quantify the average I_{int}/I_0 (all the inset images in the following figures have the same physical meaning if not otherwise indicated). The I_{int}/I_0 ratio increases quickly along with the increase of NaCl concentration. For example, it increased from 0.05 to 0.7 when the pure water was substituted by 0.025 M NaCl. This ratio is rather constant, even after incubation in salt solution for up to 12 h, demonstrating that 10 min is already long enough to reach equilibrium. And this result also confirms that the concentration of FL inside depends on the Donnan potential difference and less on the wall permeability. When the NaCl concentration was increased to 0.2 M, the same intensity was recorded from the capsule interiors and the bulk, implying free permeation of FL. The same alteration tendency in NaCl solution was recorded for FITC−dextran with a molecular weight of ~4 kDa, too (data not shown). One can thus conclude that the filling degree of negatively charged species in the capsule interior is tunable by ionic strength.

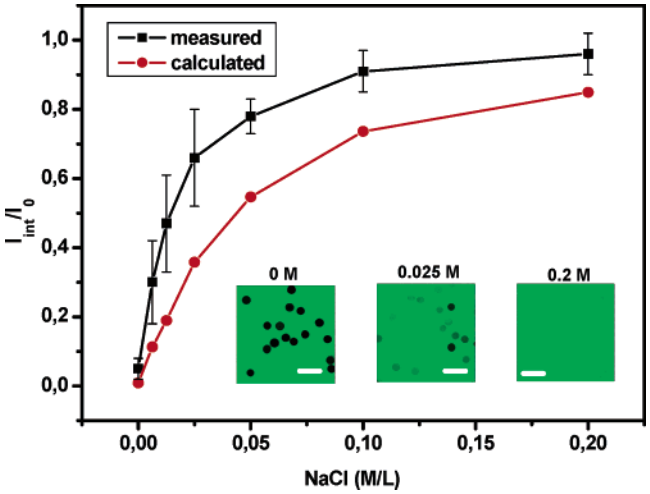

Figure 3. The measured and calculated fluorescence intensity ratio (I_{int}/I_0) between the capsule interior (I_{int}) and the bulk solution (I_0) as a function of NaCl concentration. The inset CLSM images were recorded at each NaCl concentration. Scale bar = 20 μm. The same realistic parameters and model as those employed in Figure 2 were used for the calculation.

According to the simple Donnan equilibrium model described in ref 12b combining counterion condensation, the distribution of FL as a function of bulk NaCl concentration can also be calculated, which is illustrated in Figure 3. The tendency of the variation corresponds to the experimental results: the increase of ionic strength decreases the Donnan potential and hence increases the inner FL concentration. However, the calculated values are slightly lower than those measured. Hence, the simple Donnan model here, which only considers the electrostatic interaction, is insufficient to explain the effects quantitatively, since the equilibrium distribution of the permeants between the capsule interior and bulk solution results from both electrostatic and other specific interactions.[16] As a conclusion, in our system there should be some other specific interactions between the FL and PSS molecules, for instance, the hydrophobic interaction, which can increase the FL distribution inside the capsules. Further experiments should be done to clarify this speculation.

Solvent Polarity Dependence. By mixing ethanol and water, the dielectric constant of the solvent can be easily tuned. With the decrease of solvent dielectric constant, due to the addition of the less polar ethanol, according to eq 2, the value of θ decreases. This means that addition of ethanol will lower the charge density of the PSS molecules, thus decreasing the

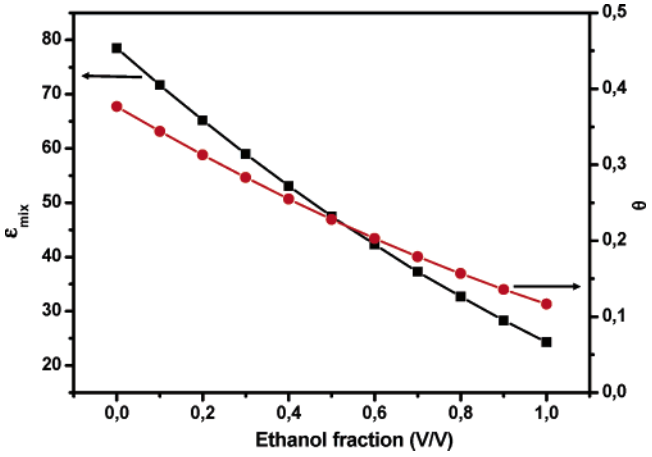

Figure 4. The calculated dielectric constant ϵ_{mix} of ethanol−water mixed solvent and the net charge fraction (θ) of the PSS backbone as a function of ethanol volume fraction according to eqs 2 and 3.

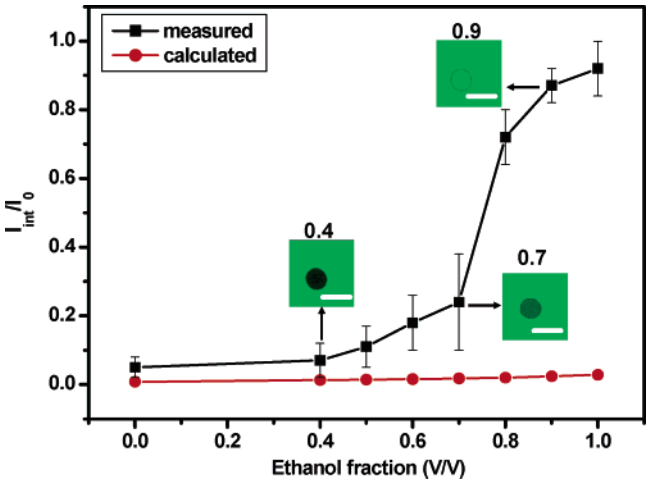

Figure 5. The measured and calculated fluorescence intensity ratio (I_{int}/I_0) as a function of ethanol volume fraction. The inset CLSM images were recorded at each ethanol volume fraction. Scale bar = 10 μm. The same realistic parameters and model as those employed in Figure 2 were used for calculation, and θ is obtained from Figure 4. The deviations between experiment and calculation can be ascribed to PSS precipitation at high ethanol content (see the text).

Donnan potential. The dielectric constant of a mixed solvent (ϵ_{mix}) can be calculated by a two-component mixing formula[17]

$$\epsilon_{mix}^{(1/2)} = \varphi_1 \epsilon_1^{(1/2)} + \varphi_2 \epsilon_2^{(1/2)} \quad (3)$$

where ϵ_1 and ϵ_2 are the dielectric constants of components 1 and 2 (78.5 for water and 24.3 for ethanol), respectively, and φ_1 and φ_2 are the respective volumetric fractions.

Figure 4 depicts the variation of ϵ_{mix} and θ as a function of ethanol volume fraction. θ changes in a relatively small range compared with ϵ_{mix}. Using the θ values and assuming that FL is in an anion form, one can roughly estimate the distribution of FL as a function of bulk ethanol fraction according to the Donnan equilibrium model in ref 12b. The result is illustrated in Figure 5. Basically, the FL should be almost completely excluded according to the calculation. However, the experimental results are different (Figure 5). The measured I_{int}/I_0 ratio increases in a comparatively slow manner and has no significant differences ($P > 0.05$) when the ethanol fraction is below 0.7, which is consistent with the calculated results. This means that in this ethanol fraction range the encapsulated charged PSS molecules clearly cause the Donnan distribution of FL. The diffusion of FL into the capsules is slowed by the electric field near and across the shell reflecting the Donnan potential difference. The slightly higher values compared with those calculated in the ethanol fraction range of 0.4−0.7 may result from the incomplete dissociation of FL and hydrophobic interaction. However, a sudden increase of the I_{int}/I_0 ratio takes place when the ethanol fraction is above 0.7 ($P < 0.05$ compared with that of an ethanol volume of 0.7), which is totally different from the calculated results. Changing the solvent polarity here has two principally different consequences: (1) the dielectric constant of the solvent influences the net charge of encapsulated PSS to induce the decrease of the Donnan potential and the effect is monotonic and changes in a small range and (2) the solvent quality may change and this may lead to a precipitation of the polyelectrolytes, since we observe an abrupt change of the fluorescence intensity with ethanol content increase. The main contribution is expected to arise from the second effect. The precipitation volume of ethanol for PSS is about 0.8, which should approximately correspond to the Θ condition of the system.[18] Approaching this point results in strongly suppressed ionization of PSS and thus significant precipitation of the polymers. Beyond 0.9, FL could freely penetrate inside the capsules, leading to the same fluorescence intensity from capsule interior and bulk. Again, no alteration of the I_{int}/I_0 ratio at each ethanol volume was observed after long-time incubation (12 h), demonstrating that the FL distribution is controlled thermodynamically rather than kinetically. It is known that the increase of ethanol concentration exceeding a definite concentration leads to the disruption of the ordered spatial structure of water and, as a result, to the formation of water-depleted associates maintained by hydrophobic interactions.[14] This effect may also be involved.

Conclusions

The influence of ionic strength and solvent polarity on the equilibrium distribution of negatively charged permeants between polyelectrolyte microcapsules having negatively charged polyelectrolyte inside and the bulk solution is systematically investigated. Negatively charged permeants such as FL and FITC−dextran are excluded by this kind of capsules due to a Donnan effect, but positively charged probes such as Rd6G and TRITC−dextran can spontaneously deposit. The Donnan potential can be decreased by addition of salt to increase the bulk ionic strength; thus, the permeant gradients across the capsule wall are reduced. The specific interactions between permeants and the encapsulated polyelectrolytes may also be important to determine the permeant distribution. Although addition of ethanol can reduce the dielectric constant of the solvent to lower the charge density of the encapsulated polyelectrolyte, as a result to decrease the Donnan potential, this effect is monotonic and changes slightly, which cannot explain the experimental results in the high ethanol fraction range. Actually, a sharp increase of the I_{int}/I_0 ratio is recorded when the ethanol volume fraction is above 0.7, which should be mainly attributed to the precipitation of entrapped polyelectrolyte. In conclusion, the inner concentration of a dye probe with a molecular weight below several kilodaltons depends on the Donnan equilibrium rather than the wall permeability. This principle can be generalized for the encapsulation of charged low molecular weight drugs that can permeate easily the capsule walls. However, they may be kept inside via local equilibrium conditions, and only changing these via ionic strength, solvent, or other additives enables a sustained release.

Acknowledgment. We thank Prof. J. C. Shen for his continuous support and stimulating discussions. W. J. Tong and C.Y. Gao thank the Max-Planck Society for a visiting scientist grant. This study is financially supported by the Natural Science Foundation of China (No. 20434030) and the National Science Fund for Distinguished Young Scholars of China (No. 50425311).

References and Notes

(1) (a) Decher, G. *Science* **1997**, *277*, 1232. (b) Donath, E.; Sukhorukov, G. B.; Caruso, F.; Davis, S. A.; Möhwald, H. *Angew. Chem., Int. Ed.* **1998**, *37*, 2202. (c) Caruso, F.; Caruso, R. A.; Möhwald, H. *Science* **1998**, *282*, 1111. (d) Peyratout, C. S.; Dähne, L. *Angew. Chem., Int. Ed* **2004**, *43*, 3762.

(2) (a) Moya, S.; Dähne, L.; Voigt, A.; Leporatti, S.; Donath, E.; Möhwald, H. *Colloids Surf., A* **2001**, *183*, 27. (b) Caruso, F.; Trau, D.; Möhwald, H.; Renneberg, R. *Langmuir* **2000**, *16*, 1485. (c) McShane, M. J.; Brown, J. Q.; Guice, K. B.; Lvov, Y. M. *J. Nanosci. Nanotechnol.* **2002**, *2*, 411. (d) Shchukin, D. G.; Sukhorukov, G. B. *Adv. Mater.* **2004**, *16*, 671.

(3) (a) For a review, see: Antipov, A. A.; Sukhorukov, G. B. *Adv. Colloid Interface* **2004**, *111*, 49. (b) Antipov, A. A.; Sukhorukov, G. B.; Donath, E.; Möhwald, H. *J. Phys. Chem. B* **2001**, *105*, 2281.

(4) (a) Tong, W. J.; Gao, C. Y.; Möhwald, H. *Chem. Mater.* **2005**, *17*, 4610. (b) Zhu, H. G.; McShane, M. J. *Langmuir* **2005**, *21*, 424.

(5) (a) Antipov, A. A.; Sukhorukov, G. B.; Leporatti, S.; Radtchenko, I. L.; Donath, E.; Möhwald, H. *Colloids Surf., A* **2002**, *198*, 535. (b) Sukhorukov, G. B.; Antipov, A. A.; Voigt, A.; Donath, E.; Möhwald, H. *Macromol. Rapid Commun.* **2001**, *22*, 44.

(6) (a) Ibarz, G.; Dähne, L.; Donath, E.; Möhwald, H. *Adv. Mater.* **2001**, *13*, 1324. (b) Antipov, A. A.; Sukhorukov, G. B.; Möhwald, H. *Langmuir* **2003**, *19*, 2444.

(7) Lvov, Y.; Antipov, A. A.; Mamedov, A.; Möhwald, H.; Sukhorukov, G. B. *Nano Lett.* **2001**, *1*, 125.

(8) Ibarz, G.; Dähne, L.; Donath, E.; Möhwald, H. *Chem. Mater.* **2002**, *14*, 4059.

(9) (a) Ibarz, G.; Dähne, L.; Donath, E.; Möhwald, H. *Macromol. Rapid Commun.* **2002**, *23*, 474. (b) Georgieva, R.; Moya, S.; Donath, E.; Baumler, H. *Langmuir* **2004**, *20*, 1895. (c) Moya, S.; Donath, E.; Sukhorukov, G. B.; Auch, M.; Baumler, H.; Lichtenfeld, H.; Möhwald, H. *Macromolecules* **2000**, *33*, 4538.

(10) (a) Dähne, L.; Leporatti, S.; Donath, E.; Möhwald, H. *J. Am. Chem. Soc.* **2001**, *123*, 5431. (b) Berth, G.; Voigt, A.; Dautzenberg, H.; Donath, E.; Möhwald, H. *Biomacromolecules* **2002**, *3*, 579. (c) Gao, C. Y.; Donath, E.; Möhwald, H.; Shen, J. C. *Angew. Chem., Int. Ed.* **2002**, *41*, 3789.

(11) Tong, W. J.; Dong, W. F.; Gao, C. Y.; Möhwald, H. *J. Phys. Chem. B* **2005**, *109*, 13159.

(12) (a) Sukhorukov, G. B.; Brumen, M.; Donath, E.; Möhwald, H. *J. Phys. Chem. B* **1999**, *103*, 6434. (b) Halo˝zan, D.; Déjugnat, C.; Brumen, M.; Sukhorukov, G. B. *J. Chem. Inf. Model.* **2005**, *45*, 1589.

(13) Manning, G. S. *J. Chem. Phys.* **1969**, *51*, 924.

(14) Hackl, E. V.; Blagoi, Y. P. *Acta Biochim. Pol.* **2000**, *47*, 103.

(15) Sjöback, R.; Nygren, J.; Kubista, M. *Spectrochim. Acta A* **1995**, *51*, L7.

(16) (a) Jaskari, T.; Vuorio, M.; Kontturi, K.; Manzanares, J. A.; Hirvonen, J. *J. Control. Release* **2001**, *70*, 219. (b) Ramírez, P.; Alcaraz, A.; Mafé, S.; Pellicer, J. *J. Colloid Interface Sci.* **2002**, *253*, 171.

(17) Starr, G. C.; Lowery, B.; Cooley, E. T. *Soil Sci. Soc. Am. J.* **2000**, *64*, 867.

(18) Poptoshev, E.; Schoeler, B.; Caruso, F. *Langmuir* **2004**, *20*, 829.